Arab J Sci Eng (2014) 39:2001–2011
DOI 10.1007/s13369-013-0731-x

RESEARCH ARTICLE - ELECTRICAL ENGINEERING

A Fixed Switching Frequency Direct Torque Control Strategy for Induction Motor Drives Using Indirect Matrix Converter

N. Taïb · B. Metidji · T. Rekioua

Received: 9 March 2012 / Accepted: 11 July 2013 / Published online: 6 September 2013

Abstract Direct torque control (DTC) is a very competitive control strategy because of its simple structure and good dynamic performance essentially in terms of torque response. However, there are some drawbacks which need to be eliminated or at least reduced, like the variable switching frequency and torque ripples. Matrix converters are the new generation of power converters which provide a very good quality of input and output waveforms with a controllability of input power factor, a bidirectional power flow and a compact sight structure. In this present paper, we propose a method used for a fixed switching frequency direct torque control (FSF-DTC) using an indirect matrix converter (IMC). This method is characterized by a simple structure, FSF-DTC which causes minimal torque ripple and unity input power factor. Using this strategy, we combine the IMCs advantages with those of DTC schemes. The technique used to obtain the constant frequency, based on a triangular waveform added to the reference of the torque to impose the dynamic of the torque slopes, is combined with the input current space vector to create the switching table for the IMC drives. The input current modulation allows the rectification stage control of the IMC, while the inverter stage is controlled using the classical DTC switching table. Simulation results clearly demonstrate a better dynamic and steady state performances of the proposed method.

Keywords Indirect matrix converter · Direct torque control · Induction motor drives · Fixed switching frequency DTC · Torque ripple reduction

N. Taïb (✉) · B. Metidji · T. Rekioua
LTII Laboratory, Electrical Engineering Department,
University A. Mira, Bejaia, Algeria
e-mail: taib_nabil@yahoo.fr

الخلاصة

يُعد التحكم المباشر لعزم الدوران (DTC) استراتيجية تحكم منافسة للغاية بسبب البنية البسيطة وديناميكية أداء جيدة للعزم. ومع ذلك، فإن هناك بعض العيوب التى تحتاج الى ازالة أو على الأقل الحد منها مثل تردد التحويل المتغيرة وتموجات العزم. إن المحولات المصفوفاتية هي الجيل الجديد من محولات الطاقة التي توفر قيمة جيدة جدا للمدخلات والمخرجات من حيث الأشكال الموجية مع إمكانية التحكم في معامل الطاقة عند المدخل، وتدفق الطاقة في الاتجاهين وقابلية تقليص حجم الهيكل. وفى هذه الورقة، نقترح طريقة تستخدم التحويل ثابت التردد للتحكم المباشرة للعزم (FSF-DTC) باستخدام محول مصفوفاتي غير مباشر (IMC). وتتميزهذه الطريقة ببنية بسيطة، وتردد التحويل ثابت (DTC) الذي يسبب الحد الأدنى في تموجات العزم ومعامل الطاقة عند المدخل بقيمة الوحدة. وباستخدام هذه الاستراتيجية نمزج بين مزايا المحولات المصفوفاتية غير المباشرة مع تلك التي تمتلكها تقنية التحكم المباشر للعزم (DTC). والأسلوب المستخدم للحصول على التردد الثابت الذي يرتكز على شكل الموجة المثلثية التي تضاف الى العزم على لفرض ديناميكية لتغيرات العزم، مع الفضاء الشعاعي لتيار الإدخال مكّننا من إنشاء جدول التحويل للمحول المصفوفاتي غير المباشر (IMC) المستعمل في النظام. ويسمح تعديل التيار عند المدخل بالتحكم في المحوّل المقوّم (IMC) ، وأمّا المحوّل العاكس يتم التحكم به باستخدام جدول التحويل (DTC) الكلاسيكية. وتدلّ نتائج المحاكاة بوضوح على مدى نجاع طريقة التحكم المقترحة انطلاقا من أفضل العروض الديناميكية والثابتة المقدّمة من النظام المدروس.

List of Symbols

V_s	Stator supply voltage vector (V)
p	Number of pole pairs
L_m	Mutual inductance (H)
L_s, L_r	Stator and rotor self-inductance (H)
σ	Total leakage factor
ϕ_s	Stator flux linkage (Wb)
ϕ'_r	Rotor flux linkage expressed in the stationary frame (Wb)
γ	Displacement angle between stator and rotor flux
T_e	Electromagnetic torque (N m)

T_{eref}	Electromagnetic reference torque (N m)
$\Delta T_{\text{e(max)}}$	Maximal torque variation (N m)
A_{tr}	Triangular waveform magnitude
f_{tr}	Triangular waveform frequency (Hz)
B_{H}	Hysteresis torque band limits
T_{tr}	Triangular waveform period (μs)
T_{c}	Switching period (μs)
d_γ, d_δ	Duty cycles for active vectors applied to rectifier stage of IMC
d'_γ, d'_δ	Resized duty cycles for active vectors applied to rectifier stage of IMC
m_{ij}	Duty cycles applied for each switch S_{ij} of the IMC
$v_{\text{i}}(t)$	Input voltages (V)
$v_{\text{o}}(t)$	Output voltages (V)
$i_{\text{i}}(t)$	Input currents (A)
$i_{\text{o}}(t)$	Output currents (A)
$M(t)$ and $M^{\text{T}}(t)$	Modulation matrix and its transpose
θ_{in}	Input current reference vector angle into a sector where it lies

1 Introduction

The AC–AC matrix converter (MC), which appeared in 1980 [1–3], has received considerable attention because of its numerous merits such as no DC-link capacitor with limited lifetime, the bi-directional power flow control, the sinusoidal input output waveforms and adjustable input power factor.

Moreover, MC is compact sight because of the lack of DC-link bus capacity used for energy storage. Comprehensive researches on MC, so far, have been focused on modulation methods [4–9], integration, protection and gate drive cost and size [10,11], and MC topologies [12,13], especially the indirect matrix converter (IMC) topology. The IMC was first proposed and also confirmed experimentally in [14] and then more attention was given to this topology [15,16]. Many applications were presented in the literature for the MC associated with the AC drives [17–19] and recently with the renewable energy systems [20].

After that, with the improvement of the hardware microcontrollers and bidirectional switches, the focus of the research will be on the applications of these kinds of converters such as variable speed drives and some other applications.

The direct torque control (DTC) methods of alternating current machines appeared in the second half of 1980 as a competitor of the traditional methods, based on PWM supplies and a decoupling of flux and torque by the magnetic field orientation control (FOC).

The DTC scheme for direct MC was initially presented in [21]. The generation of the voltage vectors required implementation of the DTC of induction motors under unity input power factor constraint that was allowed.

However, the DTC scheme using a switching table has some fatal drawbacks. The switching frequency varies according to the motor speed and the hysteresis bands of the torque and flux. A large torque ripple is generated at a low speed range because of the small back electromotive force of the induction motor and high control sampling time required to achieve good performances.

Although several methods have been presented to solve these problems [22–24], these methods are designed for a conventional inverter drive system. On the contrary, for the MC a few solutions have been presented [25], which use the direct torque controlled space vector modulated method (DTC-SVM) to build the switching table of the converter. In [26], the authors proposed using only a wider range of input voltage vectors for the MC rather than the rotating vectors to develop a new lookup table that distinguishes between small and large torque errors where the variable switching frequency has not been dealt with. For the IMC, the solutions proposed in [27,28] have not declared or studied the problem of variable switching frequency of the DTC.

In this paper, a new fixed switching frequency DTC (FSF-DTC) scheme using IMC is presented, which enables minimizing torque ripple under a unity input power factor constraint. The proposed control scheme of the FSF-DTC of an induction motor drive fed by IMC is based on the classic DTC switching table, the input voltage angle detection and a high-frequency triangular waveform. The effectiveness of the proposed control scheme is demonstrated through simulation results.

2 Description of the Global System

The well-known classic DTC method is based on the following algorithm:

- At each period, the line currents and voltages are measured.
- The stator vector flux components are constructed.
- The torque estimation may now be performed.

The flux and torque reference values are compared with their actual values, and the resulting values are fed in two-level and three-level hysteresis comparators, respectively. The outputs of both stator flux and torque comparators, respectively, (φ and τ), together with the position of the stator flux are used as inputs of the basic DTC switching lookup table (Table 1). The position of the stator flux is divided into six different sections (θ(i)) as shown in Fig. 1.

Figure 2 shows the global proposed drive scheme using the constant-frequency DTC, based on the classic table and the method described in Sect. 4 using the IMC structure shown in Fig. 3.

Table 1 Basic DTC switching table

ϕ	τ	$\theta_{(1)}$	$\theta_{(2)}$	$\theta_{(3)}$	$\theta_{(4)}$	$\theta_{(5)}$	$\theta_{(6)}$
1	1	v_2	v_3	v_4	v_5	v_6	v_1
1	0	v_7	v_0	v_7	v_0	v_7	v_0
1	−1	v_6	v_1	v_2	v_3	v_4	v_5
0	1	v_3	v_4	v_5	v_6	v_1	v_2
0	0	v_0	v_7	v_0	v_7	v_0	v_7
0	−1	v_5	v_6	v_1	v_2	v_3	v_4

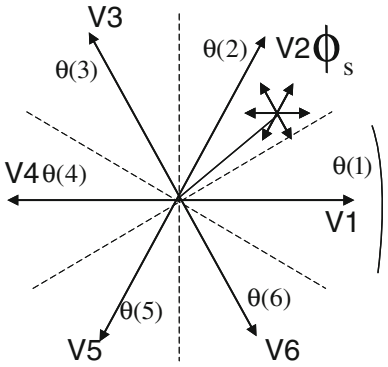

Fig. 1 VSI output line to neutral voltage vector and corresponding stator flux variation

3 Fixed Switching Frequency DTC Principles with IMC

3.1 Fixed Switching Frequency DTC Concepts

The stator flux and the electromagnetic torque expressions of an induction motor are given by (1) and (2), respectively:

$$\phi_s = \int_0^t V_s \mathrm{d}t \tag{1}$$

$$T_e = \frac{3}{2} p \frac{L_m}{\sigma L_s L_r} |\phi_s| \left|\phi'_r\right| \sin\gamma \tag{2}$$

The electromagnetic torque is a sinusoidal function of γ, the angle between ϕ_s and ϕ'_r. The magnitude of the stator flux is kept constant to be able to control the motor torque by the angle γ. The rotor time constant of the standard induction machine is typically larger than 100 ms; thus, the rotor flux is stable and variations in the rotor flux are slow compared to that of the stator flux. It is therefore possible to achieve the required torque very effectively by rotating the stator flux vector, replaced by the stator voltage vector, directly in a given direction as fast as possible.

The variable switching frequency in the basic DTC is due to the variation of the time taken for the torque error to achieve the upper and lower hysteresis band limits. The waveform and the dynamic of the torque error slopes are highly dependant on operating conditions. Consequently, the torque ripple will remain high, even with small hysteresis band limits (Fig. 4).

By assuming a fixed gradient of the electromagnetic torque 'T_e' over each sampling period, the suitable form of the reference should be triangular. So, we will superpose the torque error with high-frequency triangular waveform whose parameters are the magnitude A_{tr} and the frequency f_{tr}. These parameters mainly depend on the torque dynamic and torque hysteresis band limit B_H (Fig. 5). In this case, the esteemed torque variation during a half period of the triangular signal should not exceed the difference between the maximum of the upper limit and the minimum of the lower one, as shown in Fig. 5.

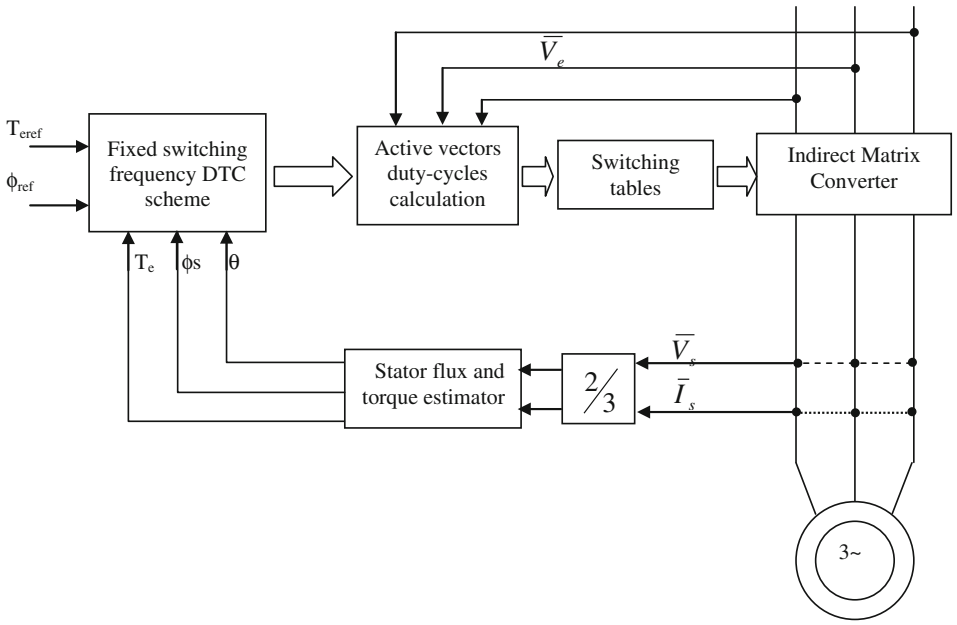

Fig. 2 The proposed fixed frequency DTC scheme for IMC drives

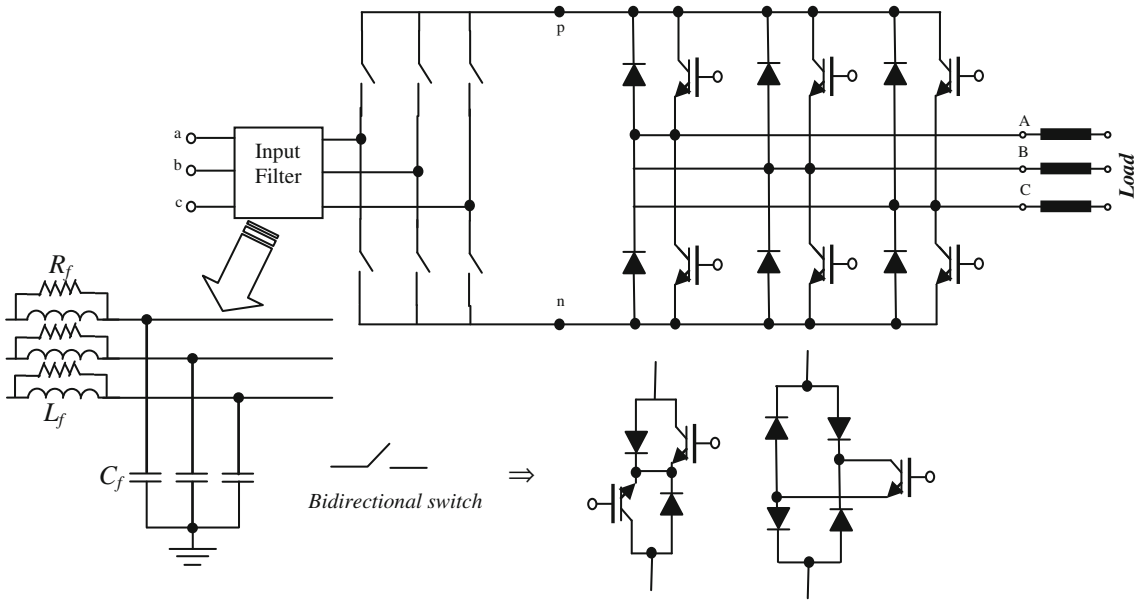

Fig. 3 Indirect matrix converter structure

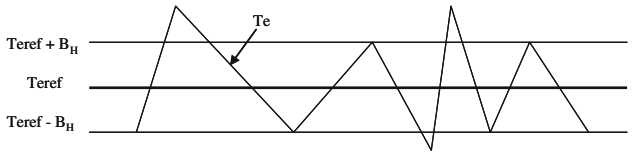

Fig. 4 Torque error causing variable switching frequency in the DTC scheme

3.2 Torque Ripples and Switching Frequency Dependencies

According to a variation of the torque slopes, the triangular parameters (magnitude A_{tr} and period T_{tr}) may be chosen under a given hysteresis band limit such as to get significant added performances. So, three situations should be considered.

- *Situation 1*: the torque slopes have slow variations (see Fig. 6a). The torque reaches the upper limit of the hysteresis band after more than one triangular period. Thus, the switching frequency will have a different value to that of the imposed triangular waveform.
- *Situation 2*: the torque slopes have quick variations (see Fig. 6b). The torque reaches the upper limit of the hysteresis band more than one time during the imposed triangular waveform period. So, switching frequency will be higher than the triangular frequency which makes it uncontrollable.
- *Situation 3*: the torque slopes have the same period as the imposed triangular one where two intersections with hysteresis band limits take place as shown in Fig. 5a.

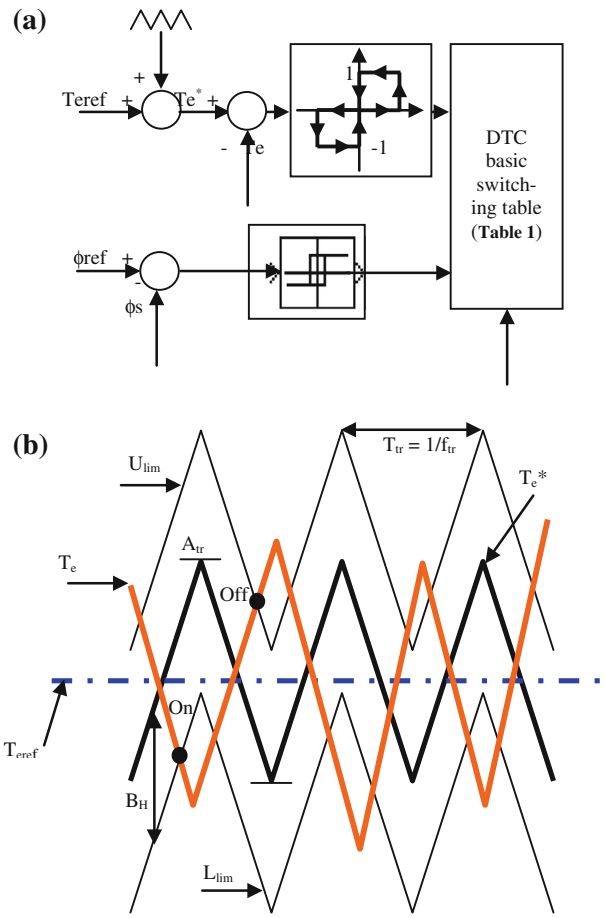

Fig. 5 **a** Proposed fixed frequency DTC scheme; **b** switches states determination

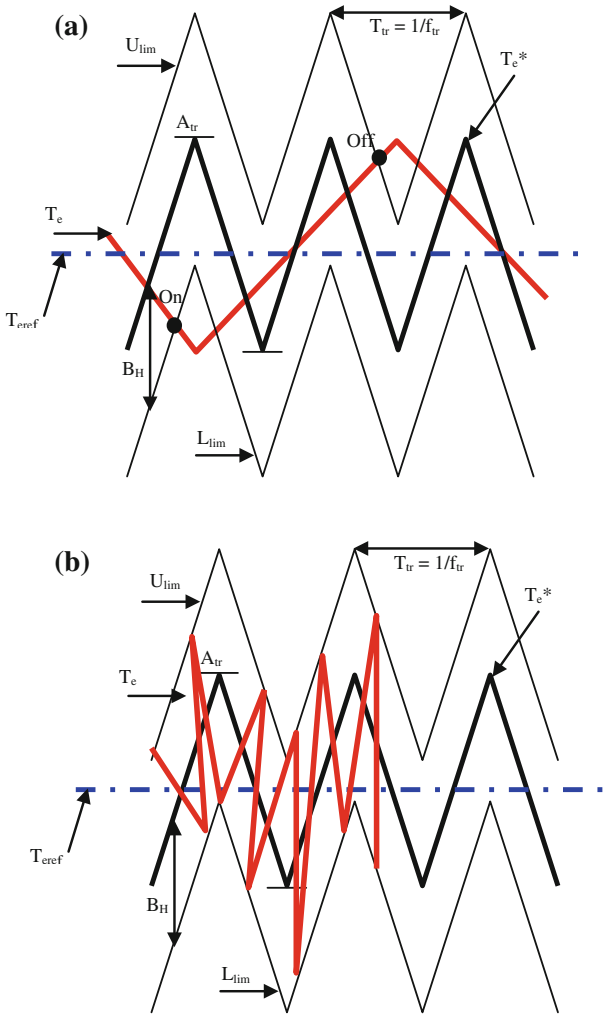

Fig. 6 Situations presented between torque slopes and triangular waveform frequency

From Fig. 5 and assuming that the triangular waveform parameters must not exceed the maximum of the electromagnetic torque variations, it can be demonstrated that:

$$\left\| \frac{\mathrm{d}T_\mathrm{e}}{\mathrm{d}t} \right\|_{\max} = \frac{\Delta T_{\mathrm{e(max)}}}{\frac{T_\mathrm{tr}}{2}} \leq \frac{4(A_\mathrm{tr} + B_\mathrm{H})}{T_\mathrm{tr}} \tag{3}$$

where T_tr is the triangular waveform period.

It is well known that we can express the electromagnetic torque in Park frame only with stator and rotor currents by (4):

$$T_\mathrm{e} = \frac{3}{2} L_\mathrm{m} \left(i_\mathrm{ds} i_\mathrm{qr} - i_\mathrm{qs} i_\mathrm{dr} \right) \tag{4}$$

Since the frequency of the rotor current is much smaller than that of the stator, it can be concluded that the dynamic of the torque is directly affected by the dynamic of the stator current and vice versa. Thus, the inductive parameters of the induction machine will mainly affect this dynamic.

3.3 Fixed Switching Frequency DTC Using Indirect Matrix Converter

From the basic DTC described in Sect. 2, it appears that the conventional switching table (Table 1) is not able to generate the full vector of signal gates, which allows the MC control, because we have nine bidirectional switches to control in the MC and each output phase can be connected to any input phase. Then, the most modulation technique used for the MC is the indirect space vector modulation (ISVM) method [4]. In this technique, we consider the MC as a two-stage power converter: the first stage is a rectifier current source and the second a voltage source inverter. So, the vector generated from Table 1 is assimilated to the SVM applied to the inverter stage of direct MC. To have full control of MC, we need to use the input current modulator for the rectification stage, as used in the (ISVM) method. We will be able to generate the switching table for direct MC.

The most used modulation for the IMCs is also the SVM [4]. Since we will use only the SVM method for the rectification stage, the space vector of the input current is defined as follows:

$$\bar{I}_i = \frac{2}{3} \left(i_a + i_b \mathrm{e}^{j\frac{2\pi}{3}} + i_c \mathrm{e}^{j\frac{4\pi}{3}} \right) \tag{5}$$

There are six possible switching vectors which can be used by the proposed FSF-DTC scheme summarized in Table 2, because in the IMC (detailed model of IMC shown in Appendix A) control strategy, the SVM is used only for the rectification stage, where the zero vectors are not used since they will be used in the inverter stage.

In principle, the proposed control technique of the IMC selects, at each sampling period, the proper switching configuration which allows the compensation of instantaneous errors of flux and torque, under the constraint of unity input power factor. This last requirement of the IMC input side is intrinsically satisfied if we assume that the reference space vector of the input current of IMC is the input voltage vector. When an active vector is selected from the DTC switching table (Table 1), which will be applied to the inverter stage, the input current reference vector lays in one of the six sectors (Fig. 7). The duty cycles are computed as in (6):

$$\begin{aligned} d_\gamma &= \sin\left(\frac{\pi}{3} - \theta_\mathrm{in}\right) \\ d_\delta &= \sin(\theta_\mathrm{in}) \end{aligned} \tag{6}$$

in which θ_in is the angle in the switching hexagon of the input current reference vector with the right axis of the sector where the reference input space current vector lies.

Since the zero vector is used in DTC to maintain the torque constant, the applied switching sequences do not include the zero sequence (000 or 111) during the switching period of

Table 2 Proposed indirect matrix converter rectification stage switching table

Input current sectors	I	II	III	IV	V	VI
γ and δ sequences	ab, ac	ac, bc	bc, ba	ba, ca	ca, cb	cb, ab

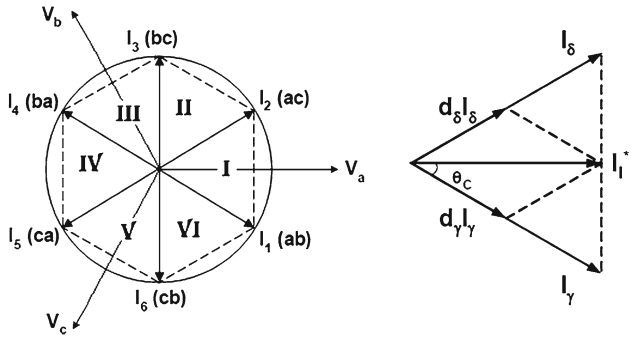

Fig. 7 Input current reference vector hexagon

the rectification stage. So, the duty cycles may be adjusted to have two vectors to apply during the whole switching period. To solve this problem, an approach is used to adjust the duty cycles.

If we assume that the new duty cycles are d'_γ and d'_δ, we can resize the duty cycles d_γ and $d_\delta$using the expressions given by (7):

$$d'_\gamma = \frac{d_\gamma}{d_\gamma + d_\delta}$$
$$d'_\delta = \frac{d_\delta}{d_\gamma + d_\delta} \tag{7}$$

To explain the implementation of the IMC switching table, we can refer to an example. If we consider that V_1 [$V_1 = (100)$] is the inverter stage output voltage vector selected by the DTC basic algorithm in a given switching period, according to the sector in which the input current reference vector is lying, we can generate the switching sequences for the rectification stage. For example, if this sector is "I", the two suitable switching vectors to apply for the rectification stage are "*ab*" and "*ac*" (Fig. 7), respectively, during the duty cycles d'_γ and d'_δ.

Finally, the duration of each sequence is calculated by multiplying the corresponding duty cycle T_γ and T_δ with the switching period as in (8):

$$T_\gamma = d'_\gamma \cdot T_c$$
$$T_\delta = d'_\delta \cdot T_c \tag{8}$$

where T_c is the switching period.

So, following the above reasoning, the switching sequences could be defined for each switching period.

4 Simulation Results and Comments

The proposed drive system was tested by digital simulation using the scheme of Fig. 2. The simulation parameters are summarized in Tables 3, 4 and 5 for induction machine, input filter of IMC (Appendix B) and the rest of the digital simulation parameters (hysteresis band limits, sampling period, triangular waveform magnitude and frequency), respectively.

4.1 Steady State Behaviour

The obtained results for 10 Nm reference torque steps and 0.9 Wb reference flux are presented in Fig. 8, where it can be seen that the magnitudes of stator flux and electromagnetic torque follow their references. Moreover, the stator current presents good waveforms as shown in Fig. 9 where only the fundamental harmonic component is present. Thus, good performances of the drive system with regard to the FSF-DTC technique implementation are reached.

The form of the unfiltered and filtered input current in Fig. 10 is also good. The validity of the proposed strategy is confirmed as the operation of the converter is at unity input power factor. It offers also the advantage of carrying out a minimal number of switching states as well as a cells switching frequency, about 4 kHz lower than that with the conventional DTC, which can be higher than 20 kHz.

Figure 11 shows that the stator flux trajectory is circular, which also confirms the validity of the proposed technique.

Table 3 Induction motor parameters

Stator resistor, R_s	4.85 Ω
Stator inductance, L_s	0.274 mH
Rotor resistor, R_r	3.805 Ω
Rotor inductance, L_r	0.274 mH
Mutual inductance, L_m	0.258
Output power	3.5 kW
Pole pairs	2
Voltage/frequency	380 V/50 Hz

Table 4 Input filter parameters

Dumping resistor, R_f	3 Ω
Inductance, L_f	1.2 mH
Capacitor, C_f	22 μF

Table 5 Digital simulation parameters

Sampling period	50 μs
Hysteresis band limits, B_H	5 % nominal values
Triangular waveform amplitude, A_{tr}	5 % of T_e (nominal)
Triangular waveform frequency, f_{tr}	1–10 kHz

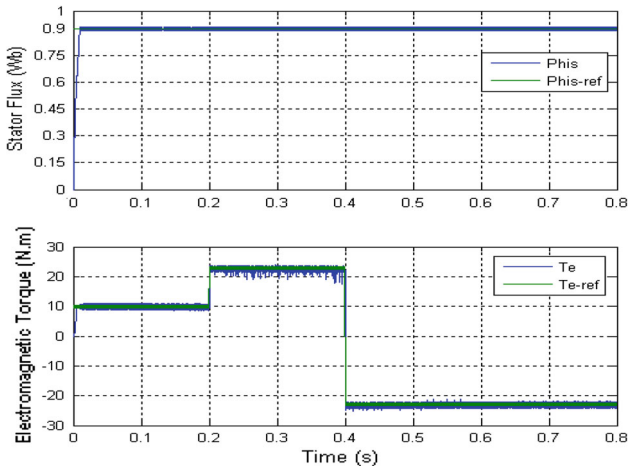

Fig. 8 Flux and torque response with the proposed DTC scheme

4.2 Dynamic Behaviour

The dynamic performances of the proposed control method are tested for a step torque command from +10 to +23 Nm and from +23 to −23 Nm as shown in Fig. 12. It can be seen that the inversion of the stator current is obtained after the step command as shown in Fig. 9.

The change in the input current direction in case of an inversion of machine speed direction at 0.4 s is shown in Fig. 9. So, in these conditions the IMC generates electric power to the grid with closely sinusoidal waveforms and unity input power factor. This demonstrates the bidirectional power flow of the IMC.

Figure 13 shows the variations of the torque at a steady state of the system. We can see that the torque has minimal fluctuations with regard to its reference, which confirms the minimization of the torque ripples. In addition, we can see the effect of the application of the two vectors or sequences at each segment of the triangular reference torque waveform.

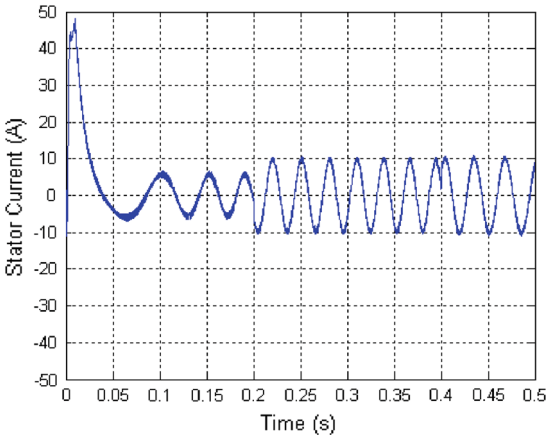

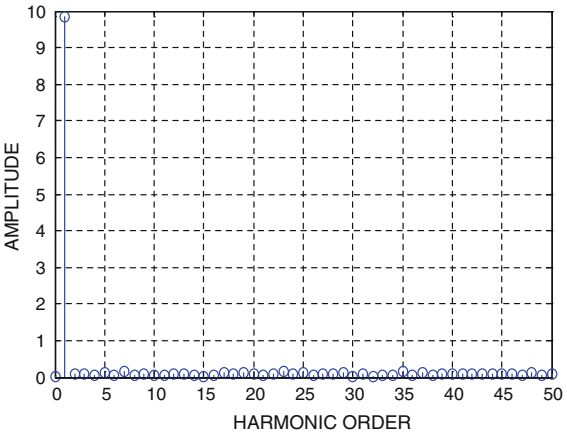

Fig. 9 Stator current waveform and its spectrum

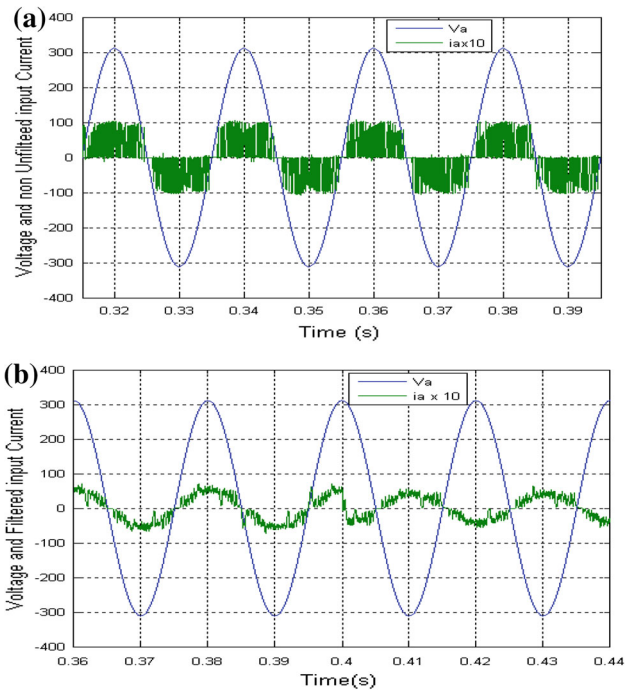

Fig. 10 Input phase voltage and current of IMC. **a** Unfiltered current; **b** filtered current

Figure 14 shows the DC-link voltage given by the IMC rectification stage with the line-to-line voltage given by the IMC inverter stage. We can see the good waveform of these voltages and this shows the effectiveness of the proposed method.

4.3 Output and Input IMC Current Quality Analysis

When the switching frequency is chosen, the total harmonic distortion (THD) of the output current of the MC current and then that of the input current should be considered under constant hysteresis band limits and magnitude of the triangular waveform.

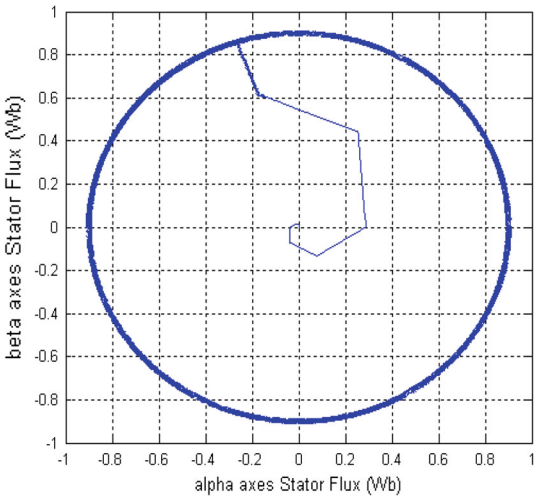

Fig. 11 Stator flux in a polar coordinate

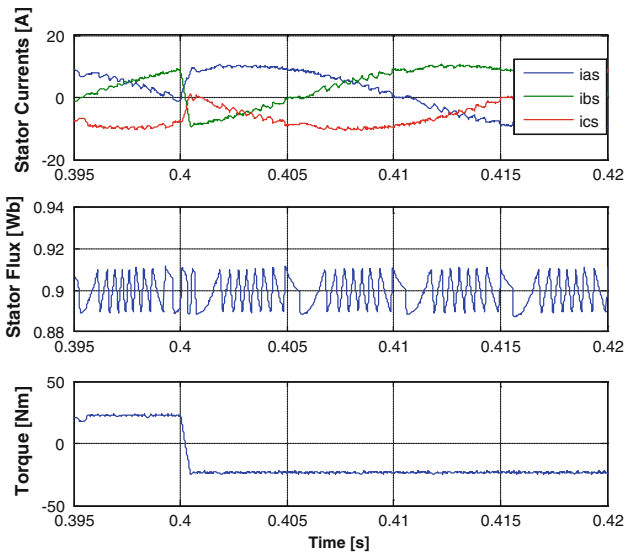

Fig. 12 Stator currents, stator flux and electromagnetic torque in the dynamic state

Varying the frequency from 1 to 10 kHz is considered to calculate the THD of the input and output IMC current. As shown in Fig. 15a, the quality of the stator current is moderately affected by the switching frequency, where this frequency is the same as that of the triangular waveform, as known. When the switching frequency is low (between 1 and 5 kHz), the stator current presents high THD, about 10.38 %, but also with acceptable values, while at high switching frequency (between 6 and 10 kHz) the THD value decreases until 6.49 % at 10 kHz which is better than 21.09 % obtained in [26]. This modification of the waveform quality of the stator current is caused by the relation between the torque and the current in the induction machines. At constant stator flux, the stator current dynamic can be assimilated to that of the electromagnetic torque.

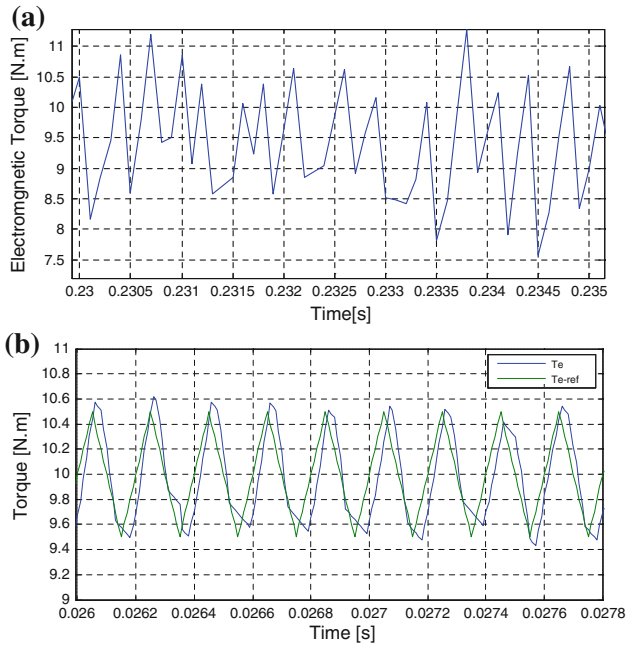

Fig. 13 Electromagnetic torque variations; **a** classic (without fixing switching frequency); **b** proposed

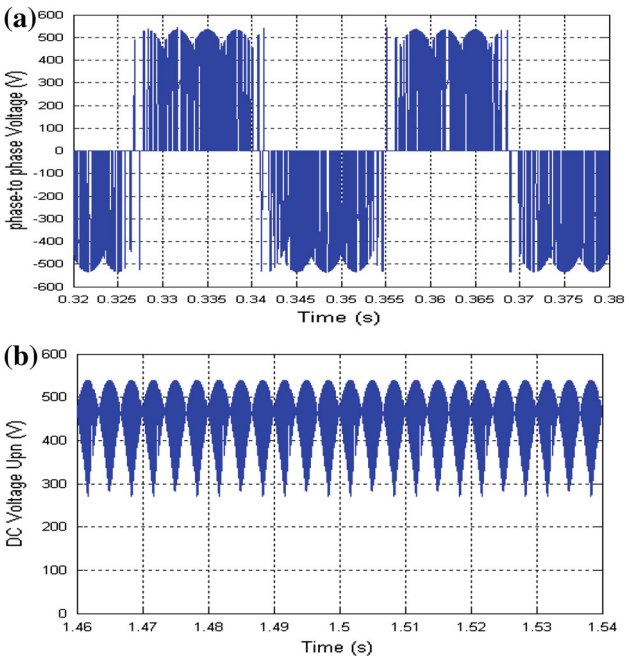

Fig. 14 **a** Line-to-line voltage and **b** DC voltage of IMC from the proposed fixed frequency DTC

For the input IMC current, its quality is slightly affected by the switching frequency imposed on the DTC control system (Fig. 15b). This low sensitivity is caused by the inserting of the LC low-pass filter at the input side of the IMC which permits only the flowing of the low-frequency currents where the others are filtered.

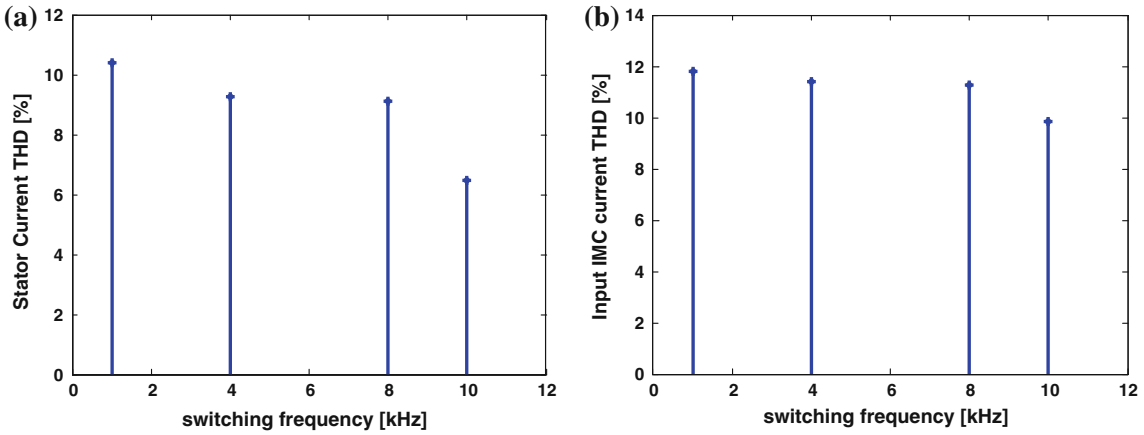

Fig. 15 THD of currents with regard to switching frequency **a** output IMC current; **b** input IMC current

5 Conclusion

An FSF-DTC of induction motor drives in which the IMC is used for supplying the system is proposed. A switching table, on the requirement basis of the machine control and those of the converter, has been defined. The advantages of the IMCs on traditional VSI-PWM are combined with those of constant-frequency DTC technique to give better performances for the induction motor drives.

The proposed control scheme has been tested as well in the steady state as in dynamic transients. The torque, the flux and current waveforms emphasize the effectiveness of the control scheme in terms of controlling the dynamic of the torque and reducing its ripples even though it presents a limitation linked to the maximum and minimum torque dynamic, which is in relation directly with the inductive parameters of the induction machine and the speed level. The results show that during regenerative breaking, the drive system acts nearly sinusoidal under unity input power factor generator. The use of IMC allows also extension to multi-machines systems, since the DC bus exists in that structure of MCs as it is very useful in electric vehicles.

Appendix A

The three-phase IMC or two-stage three-phase MC represented in Fig. 3 is an AC–DC–AC converter without resonant circuit in the DC-link part. As known, in the conventional matrix converter (CMC) there are nine bidirectional switches which allow connecting any output phase to any input phase. In the IMC, which is a cascaded connection of two bridge converters, one is the AC voltage-source rectifier (AC-VSR) and the other a DC voltage-source inverter (DC-VSI).

The AC-VSR rectifies the line-to-line AC input voltages, impressed from three-phase mains side, and generates a switched DC voltage, which is directly the input voltage for the DC-VSI. The DC-VSI inverts this impressed DC voltage and generates a switched three-phase sinusoidal AC voltage at the load side. This voltage gives rise to a sinusoidal three-phase AC current, in which ripples are limited by the serial leakage inductance of the load in case of a motor.

The basic IMC control consists of separating the control of each stage, of course taking into consideration the connection between them since they work together. The description is as follows:

For the rectifier stage, the input and output voltages are given by the relationship shown in A.1:

$$\begin{bmatrix} v_p \\ v_n \end{bmatrix} = \begin{bmatrix} m_{ap} & m_{bp} & m_{cp} \\ m_{an} & m_{bn} & m_{cn} \end{bmatrix} \cdot \begin{bmatrix} v_a \\ v_b \\ v_c \end{bmatrix} \tag{A.1}$$

For the inverter stage, the voltages relationship is given by A.2:

$$\begin{bmatrix} v_A \\ v_B \\ v_C \end{bmatrix} = \begin{bmatrix} m_{pA} & m_{nA} \\ m_{pB} & m_{nB} \\ m_{pC} & m_{nC} \end{bmatrix} \cdot \begin{bmatrix} v_p \\ v_n \end{bmatrix} \tag{A.2}$$

So, the relation between the output and input voltages of the IMC is derived from A.1 and A.2 as:

$$\begin{bmatrix} v_A \\ v_B \\ v_C \end{bmatrix} = \begin{bmatrix} m_{pA} & m_{nA} \\ m_{pB} & m_{nB} \\ m_{pC} & m_{nC} \end{bmatrix} \cdot \begin{bmatrix} m_{ap} & m_{bp} & m_{cp} \\ m_{an} & m_{bn} & m_{cn} \end{bmatrix} \cdot \begin{bmatrix} v_a \\ v_b \\ v_c \end{bmatrix} \tag{A.3}$$

where m_{ij} are the duty cycles applied for each switch S_{ij} in the two stages.

The IMC is fed by the voltage source; so, the input terminal should not be shorted. On the other hand, the load has generally an inductive nature; thus, the output phase must never be

opened. The output phase voltages $v_o(t)$ and the input phase currents $i_i(t)$ are defined by A.4 and A.5 as follows:

$$v_o(t) = M(t) \cdot v_i(t) \tag{A.4}$$

$$i_i(t) = M^T(t) \cdot i_o(t) \tag{A.5}$$

where $M(t)$ and $M^T(t)$ are, respectively, the duty cycles matrix and its transpose.

Appendix B

There are many types of filters proposed for MCs. All these filters are based on L–C components. Some of them integrate a dumping resistor. The basic design method is the resonance frequency given by:

$$f_{\text{cut-off}} = \frac{1}{2\pi\sqrt{L_f \cdot C_f}} \tag{B.1}$$

When the damping resistor R_f is used, another parameter should be considered which is a damping factor δ.

$$\delta = \frac{1}{2R_f}\sqrt{\frac{L_f}{C_f}} \tag{B.2}$$

Other considerations should be taken like the displacement factor φ_{in} between the input voltage and current throughout the power range, and the accepted voltage drop caused by the inductor L_f.

$$\cos\varphi_{\text{in}} > 0.9 \text{ for } P_{\text{out}} > 10\,\% P_{\text{nom}} \tag{B.3}$$

P_{out}, P_{nom} output and nominal MC power.

$$\tan\varphi_{\text{in}} > \frac{V_g \omega_i C_f}{0.1\frac{P_{\text{out}}}{3V_i}} \tag{B.4}$$

V_g, V_i and ω_i grid and output filter voltage, respectively, and input frequency.

Considering a small resonance frequency less than 500 Hz (about 300 Hz), unity input power factor and a motor parameter lead to make a choice of the parameters summarized in Table 4.

References

1. Venturini, M.G.B.: A new sine wave in sine wave out conversion technique which eliminates reactive elements. In: Proceedings of the Powercon'80 Conference vol. 7, pp. E3-1–E3-15 (1980)
2. Venturini, M.G.B.; Alesina, A.: The generalized transformer: a new bidirectional sinusoïdal waveform frequency converter with continously adjustable input power factor. In: Proceeding of the PESC Conference Record, pp. 242–252 (1980)
3. Alesina, A.; Venturini, M.G.B.: Analysis and design of optimum-amplitude nine-switch direct AC–AC converters. IEEE Trans. Power Electron. **4**(1), 101–112 (1989)
4. Huber, L.; Borojevic, D.: Space vector modulator for forced commutated cycloconverter. IEEE Ind. Appl. Soc. Annu. Meet. **1**, 871–876 (1989)
5. Klumpner, C.; Nielsen, P.; Boldea, I.; Blaabjerg, F.: A new matrix converter-motor (MCM) for industry applications. In: Proceeding of the IAS'00, vol. 3, pp. 1394–1402 (2000)
6. Babaei, E.; Hosseini, S.H.; Gharehpetian, G.B.: Reduction of THD and low order harmonics with symmetrical output current for single-phase ac/ac matrix converters. Int. J. Electr. Power Energy Syst. **32**(3), 225–235 (2010)
7. Nguyen, H.M.; Lee, H.H.; Chun, T.W.: Input power factor compensation algorithms using a new direct-SVM method for matrix converter. IEEE Trans. Ind. Electron. **58**(1), 232–243 (2011)
8. Hojabri, H.; Mokhtari, H.; Chang, L.: A generalized technique of modeling, analysis, and control of a matrix converter using SVD. IEEE Trans. Ind. Electron. **58**(3), 949–959 (2011)
9. Cárdenas, R.; Peña, R.; Wheeler, P.; Clare, J.: Experimental validation of a space-vector-modulation algorithm for four-leg matrix converters. IEEE Trans. Ind. Electron. **58**(4), 1282–1293 (2011)
10. Zhou, P.; Sun, K.; Liu, Z.; Huang, L.; Matsuse K.; Sasagawa, K.: A novel driving and protection circuit for reverse-blocking IGBT used in matrix converter. IEEE Trans. Ind. Appl. **43**(1), (2007)
11. Taïb, N.; Metidji, B.; Rekioua, T.; Francois, B.: Novel low cost self-powered-solution of bidirectional switch gate driver for matrix converters. IEEE Trans. Ind. Electron. **59**(1), 211–219 (2012)
12. Kolar, J.W.; Baumann, M.; Schafmeister, F.: Novel three-phase AC–DC–AC sparse matrix converter. In: Proceeding of the APEC'01, vol. 2, pp. 777–791 (2002)
13. Klumpner, C.; Wheeler, P.; Blaabjerg, F.: Control of a two stage direct power converter with a single voltage sensor mounted in the intermediary circuit. In: 35th Annual IEEE PESC'04, pp. 2385–2392 (2004)
14. Minary, Y.; Shinohara, K.; Ueda, R.: PWM-rectifier/voltage-source inverter without DC link components for induction motor drive. In: IEE Proceedings-B, vol. 140, pp. 363–368 (1993)
15. Iimori, K.; Shinohara, K.; Tarumi, O.; Fu, Z.; Muroya, M.: New current-controlled PWM rectifier-voltage source without DC link components. In: IEEE Proceeding of the 1997 IEEE Power Conversion Conference, PCC'97, Nagaoka, 23 August 1997, vol. 2, pp. 783–786 (1997)
16. Zwimpfer, P.; Stemmler, H.: Modulation and realization of a novel two-stage matrix converter. In: IEEE Proceeding of the 2001 Brazilian Power Electronics Conference, COBEP 2001, Florianpolis, 11–14 November 2001, vol. 2, pp. 485–490 (2001)
17. Gupta, R.K.; Mohapatra, K.K.; Somani, A.; Mohan, N.: Direct-matrix-converter-based drive for a three-phase open-end-winding AC machines with advanced features. IEEE Trans. Ind. Electron. **57**(12), 4032–4042 (2010)
18. Cruz, S.M.A.; Ferreira, M.; Mendes, A.M.S.: Analysis and diagnosis of open-circuit faults in matrix converters. IEEE Trans. Ind. Electron. **58**(5), 1648–1661 (2011)
19. Taïb, N.; Rekioua, T.; François, B.: An improvement fixed switching DTC induction machine fed by matrix converter. Int. J. Comput. Sci. Inf. Secur. (IJCSIS) **7**(3), 198–205 (2010)
20. Ghedamsi, K.; Aouzellag, D.: Improvement of the performances for wind energy conversions systems. Int. J. Electr. Power Energy Syst. **32**(9), 936–945 (2010)
21. Casadei, D.; Serra, G.; Tani, A.: The use of matrix converters in direct torque control of induction machines. IEEE Trans. Ind. Electron. **48**(6), 1057–1064 (2001)
22. Buja, G.S.; Kazmierkowski, M.P.: Direct torque control of PWM inverter-fed AC motors—a survey. IEEE Trans. Ind. Electron. **51**(4), 744–757 (2004)
23. Idris, N.R.N.; Yatim, A.H.M.: Direct torque control of induction machines with constant switching frequency and reduced torque ripple. IEEE Trans. Ind. Electron. **51**(4), 758–767 (2004)

24. Rekioua, D.; Rekioua, T.: Study of direct torque control strategy with minimization torque ripple for permanent magnets synchronous machines. J. Electr. Eng. **5**(1), (2005)
25. Lee, K.B.; Blaabjerg, F.: A novel unified DTC-SVM for sensorless induction motor drives fed by matrix converter. IEEE, (2005)
26. Ortega, C.; Arias, A.; Blacells, J.; Asher, G.M.: Improved waveform quality in the direct torque control of matrix-converter-fed PMSM drives. IEEE Trans. Ind. Electron. **57**(6), 2101–2110 (2010)
27. Chen, X.; Kazerani, M.: A new direct torque control strategy for induction machine based on indirect matrix converter. In: IEEE ISIE Proceeding, 9–12 July 2006, Quebec, pp. 2479–2484
28. Li, Y.; Liu, W.: A novel direct torque control method for induction motor drive system fed by two-stage matrix converter with strong robustness for input voltage. In: Second IEEE Conference on Industrial Electronics and Applications, pp. 698–702 (2007)